CLASSIFICATION OF VOLCANIC ASH USING VIIRS SENSOR DATA

Diana M. RODRIGUEZ[1], Luciano Vidal [1], Soledad OSORES[1]

[1] National Meteorological Service- ARGENTINA Mail: dmr@smn.gob.ar

ABSTRACT

The dispersion of volcanic ash in the atmosphere, caused by eruptions or subsequent resuspension of volcanic ash deposits, causes environmental impacts and affects human activities at different scales. Through remote sensors mounted on board satellites, it is possible to monitor and track volcanic ash clouds. This work presents a satellite based algorithm using three infrared bands of the VIIRS sensor on board the NOAA-20 satellite for the classification of pixels with volcanic ash, taking as a case study the eruption of the Ubinas Volcano on July 19, 2019 in Perú. These results could contribute as a tool for analysis and verification in the Buenos Aires Volcanic Ash Advisory Center (VAAC).

MOTIVATION

In the last decades, methodologies for volcanic ash classification have been developed by combining thermal bands using instruments on of board different satellites that were evaluated for different volcanic eruptions (Rose et al., 2001; Dean et al., 2003; Tupper et al., 2004). The objective of this work is to present an improved methodology for the classification of volcanic ash pixels from 3 polar satellite-based thermal bands for further automation. The analysis focuses on the ash cloud associated with the eruption of Ubinas volcano (Perú) occurred in 2019.

DATA AND METHODOLOGY

- Data: NOAA-20 VIIRS, Date: July 19, 2019 at 17:56 UTC. From : CLASS NOAA
- M Bands: M14 (8.55 µm), M15 (10.763 µm) and M16 (12.013 µm) to create BTD M15-M16 and BTD M14-M15.
- The 3-band thermal methodology proposed by Guéhenneux et al. (2015) was adapted for the VIIRS sensor and was compared with the 2-band or split window method.
- Support of the methodology: RGB True Color (Fig. 1) and RGB Ash (Fig. 4a).
- Transect generation: to determine thresholds in the classification. (Fig. 2) and (Fig. 3).
- Pixels with ash presence were identified, and a Boolean algorithm based on BTDs was used for classification.
- Three classification experiments were performed with the objective of minimizing false alarms.

RESULTS

- Thresholds used for the 3 classification methods (Tables 1 to 3).
- The M3B1 image (Fig. 4c) shows an improvement over M2B (Fig. 4b) by reducing false detections outside the blue polygon, although it did not consider inside the polygon some detected pixels and added some pixels classified as ash outside.
- Image M3B2 adds a condition and improves the classification method.

TABLE 1: *M2B* THRESHOLDS

CATEGORY	CONDITION
ASH	$BTD_{M15-M16} < 0K$
NO ASH	$BTD_{M15-M16} \geq 0K$

TABLE 2: *M3B1* THRESHOLDS

CATEGORY	CONDITION 1	CONDITION 2
ASH	$BTD_{M15-M16} \leq -0.6K$	$BTD_{M14-M15} \geq -9K$
NO ASH	$BTD_{M15-M16} > -0.6K$	$BTD_{M14-M15} < -9K$

TABLE 3: *M3B2* THRESHOLDS

CATEGORY	CONDITION 1	CONDITION 2
ASH 1	$BTD_{M15-M16} \leq -0.6K$	$BTD_{M14-M15} \geq -9K$
ASH 2	$-0.6K < BTD_{M15-M16} \leq +0.1K$	$BTD_{M14-M15} \geq -1.2K$
NO ASH	$BTD_{M15-M16} > +0.1K$	$BTD_{M14-M15} < -9K$

Fig. 1 *RGB True color [M4,M5,M6]. NOAA-20 VIIRS for 19 July 2019 at 17:56 UTC. The location of Ubinas Volcano is indicated by a red triangle.*

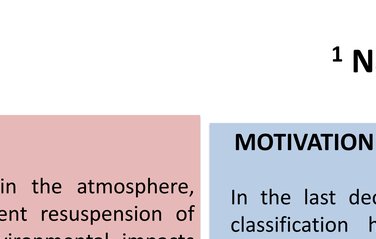

Fig. 2 *BTD difference between the M15 and M16 bands corresponding to NOAA-20 VIIRS for July 19 2019 at 17:56 UTC. The analyzed transects **T1**, **T2**, and **T3** are indicated in yellow. The letters **A** and **B** indicate the start and end of the transect.*

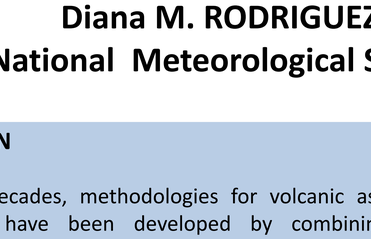

Fig. 3 Idem Fig. 2 *for the difference of M14 and M15 bands.*

(a) RGB ASH

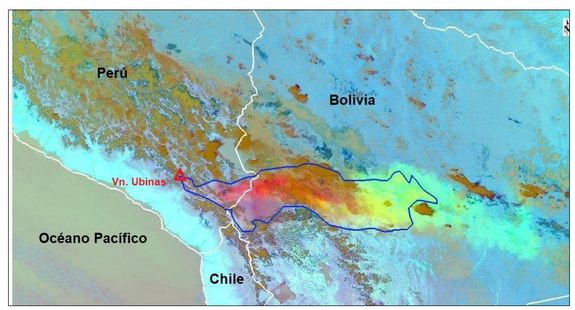

(b) Method M2B

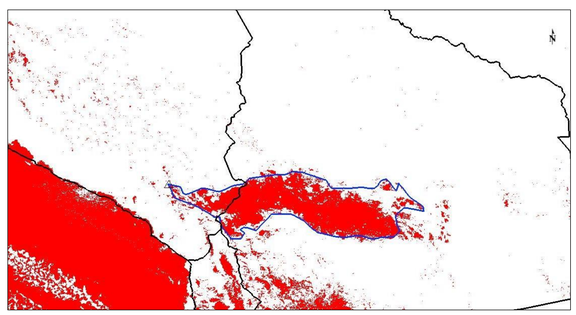

(c) Method M3B1

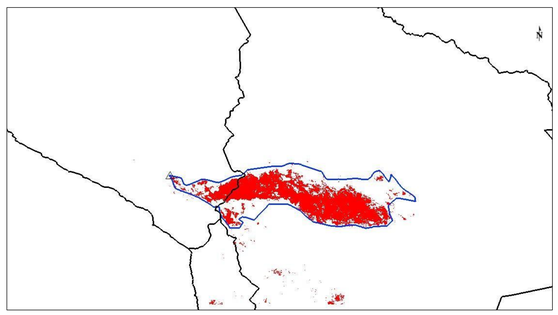

(d) Method M3B2

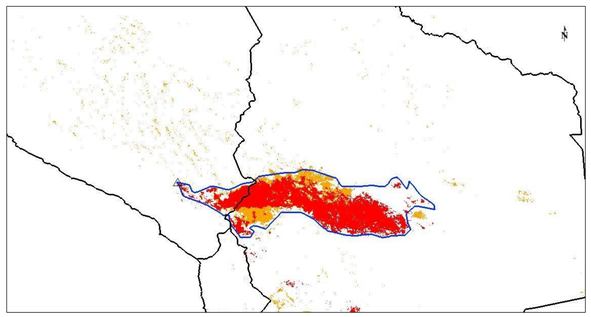

Figure 4: **(a)** NOAA-20-VIIRS, RGB ASH for 19/7/2019 at 17:56 UTC. The location of Ubinas Volcano is indicated by a red triangle. In blue outline is marked the edge of the volcanic ash cloud as determined visually by an expert. **(b)** Method M2B. **(c)** Method M3B1. **(d)** Method M3B2. Category ASH 1 is shown in red while Category ASH 2 is shown in orange.

CONCLUSIONS

The results found are encouraging, the 3-band method (M3B2) is the best performing as it includes most of the pixels visually classified as ash and discards most of the false detections. The determination of the classification threshold values is difficult since the BTD M15-M16 signal is amplified or diminished due to the low contrast of the arid and/or desert soil characteristic of this region of the Andes Mountains. To advance in a future implementation of the algorithm, it is necessary to increase the number of events to give greater robustness to the results.

REFERENCES

Dean, K.G., Dehn, J., Papp, K., Smith, S., Izbekov, P., Peterson, R., Kearney, C., Steffke, A., 2003: Integrated satellite observations of the 2001 eruption of Mt Cleveland Alaska. J. Volcano1. Geotherm. Res. 135, 51–73, http://dx.doi.org/10.1016/j.jvolgeores.2003.12.013.

Guéhenneux, Y., Gouhier, M., Labazuy, P., 2015: Improved space borne detection of volcanic ash for real-time monitoring using 3-Band method. Journal of Volcanology and Geothermal Research, 293, 25-45.

Osores, S., Toyos, G., Pujol, G., Ruiz, J., Collini, E., Folch, A., 2015: Mass loadings of the 2011 Cordón Caulle volcanic ash clouds. A quantitative comparison between MODIS and numerical simulations. IUGG-IAVCEI General Assembly. Praga.

Prata, A.J., (1989a): Observations of volcanic ash clouds using AVHRR-2 radiances. Int. J. Remote Sens. 10 (4–5), 751–761, http://dx.doi.org/10.1080/01431168908903916.

Prata, A.J., (1989b): Radiative transfer calculations for volcanic ash clouds. Geophys. Res. Lett. 16 (11), 1293–1296, http://dx.doi.org/10.1029/GL016i011p01293.

Rodríguez, D.M., Bolzi C., Rossi Lopardo, M.S., Osores, S., Maciel, S., 2019: Assay of satellite methodology for volcanic ash classification: Calbuco volcano case. AMS 100 2019 Joint Satellite Conference, September 28 - October 04, 2019 Boston, USA.

Tupper, A., Carn, S., Davey, J., Kamada, Y., Potts, R., Prata, F., Tokuno, M., 2004: An evaluation of volcanic cloud detection techniques during recent significant eruptions in the western 'Ring of Fire'. Remote Sens. Environ. 91, 27–46, http://dx.doi.org/10.1016/j.rse.2004.02.004.